Proceedings of the 8th IEEE Mediterranean Conference
on Control and Automation (MED 2000)
Rio, Patras, GREECE 17-19 July, 2000

# SLIDING MODE BASED OUTER CONTROL LOOP FOR SENSORLESS SPEED CONTROL OF PERMANENT MAGNET SYNCHRONOUS MOTOR

**JAN VITTEK***, **STEPHEN J. DODDS****, **JURAJ ALTUS***, **ROY PERRYMAN****

*University of Zilina, Faculty of Electrical Engineering, Dept. of Electric Traction and Energetic, Velky Diel, 010 26 Zilina, Slovak Republic, e-mail: vittek@fel.utc.sk, altus@fel.utc.sk
**University of East London, School of Electrical and Manufacturing Engineering, Longbridge Road, Dagenham, Essex, RM8 2AS, United Kingdom, e-mail: s.j.dodds@uel.ac.uk, r.perryman@uel.ac.uk

**Abstract:** To improve robustness to parameter uncertainties and external load torque of shaft sensorless electrical drives employing permanent magnet synchronous motors (PMSM) with forced dynamics a new more complex control system is presented. The original control structure consists of the inner loop, which is stator current control loop and the middle loop, which is shaft sensorless speed control loop based on the forced dynamics. This control structure is completed with the outer loop, based on the sliding mode control (SMC) principles. The forced dynamics control, as well as converting the non-linear PMSM into a linear element, offers higher robustness than conventional shaft sensorless speed control methods. Based on feedback linearisation a first order linear closed-loop response to speed demands with a user specified time constant is obtained. Simulation and experimental results presented show good correspondence with theoretical predictions.

**Key Words:** Synchronous motor control, observers, sliding-mode control, variable-structure control, cascade control, non-linear systems, feedback linearisation.

## 1. INTRODUCTION

In recent years „*sensorless*“ or „*self-sensing*“ control of AC machines has been extensively researched. The driving force behind this activity is to decrease total drive cost and to improve its reliability, when mechanical sensor and its connection cables are eliminated for the measurement of velocity feed-back loop.

Presented new control method of electric drives employing PMSM with forced closed-loop first order dynamics is based on feedback linearisation [9], vector control [1], [2] and sliding mode control [11]. The original forced dynamics control method of PMSM drive was introduced in [4]. The system operates without shaft sensors, only the stator currents being measured, the applied stator voltages being determined by the computed inverter switching algorithm and with a knowledge of the DC link voltage. The prescribed response to the reference speed demand was chosen as linear first order dynamics, together with the condition of vector control. Fig. 1. shows the original PMSM drive control system with forced dynamics control which contains, a set of two observers for estimation of the rotor speed and the load torque using the corresponding magnetic flux components from a flux computation algorithm.

Forced dynamics control is applicable in many non-linear multivariable automatic control applications and originally was developed for electrical drives employing induction motors [3] and later applied also for electric drives with PMSM [5] where also special arrangements of the block producing unit vectors for transformation into synchronous speed reference frame was described. First preliminary experimental

results were reported in [6] and the basic concept of outer loop improvement of the PMSM with forced dynamics was presented in [9]. The drive presented here would be very convenient also as an inner speed control loop for a position servo-system [8].

Since the control law itself, the magnetic flux calculator, the rotor angular speed observer and load torque observer are all model-based, i.e., dependent on estimates of the motor parameters, then some sensitivity to the errors in these estimates would be expected. It means that the closed-loop performance of the whole control system is affected by the errors in the aforementioned estimates. To reduce this sensitivity the intention here is to close a simple sliding mode control based loop around the original close-loop system and to improve the robustness of the complete control system. The block scheme of overall control system completed with this outer loop is shown in Fig. 2.

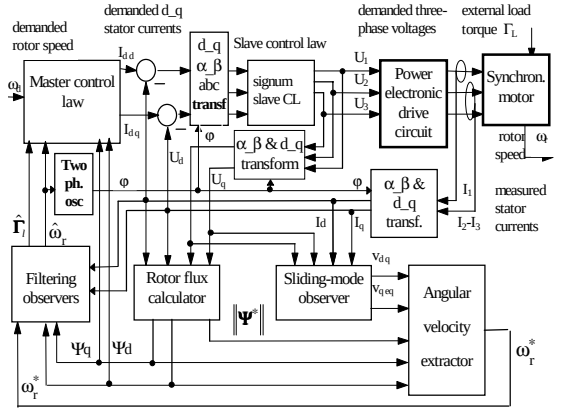


Fig. 1. Original control system of shaft sensorless speed controlled electric drive with PMSM and forced dynamics.

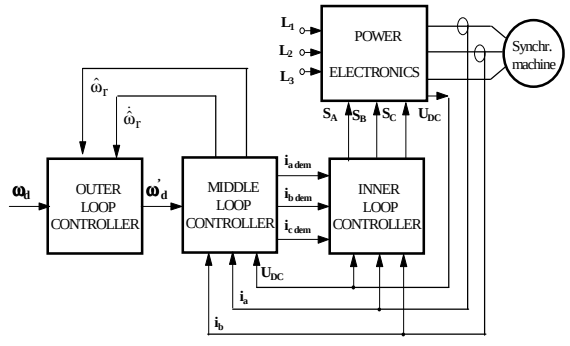


Fig. 2. Modified block scheme of the overall control system of shaft sensorless speed controlled PMSM drive with SMC based outer lop.

## 2. CONTROL SYSTEM

### 2.1. The middle loop controller

Essential for the forced dynamics control law realisation is middle loop controller. This controller forces the PMSM angular speed estimate, $\hat{\omega}_r$, to follow the speed demand, $\omega'_d$, from the outer loop controller with a linear, first order dynamics lag, value of which can be chosen as time constant, $T_1$. The middle loop controller also contains rotor speed and load torque estimation algorithms, which are obtained using the measured stator currents, $i_a$, $i_b$, and $i_c$, together with the measured voltage of the DC supply and the computed stator voltages, $u_a$, $u_b$, and $u_c$, from inverter switching algorithm.

**Model of Motor and Load.** The PMSM is described in the d-q rotating co-ordinate system fixed to the rotor of PMSM:-

$$\frac{d}{dt}\begin{bmatrix} i_d \\ i_q \end{bmatrix} = \begin{bmatrix} -\frac{R_S}{L_d} & p\omega_r \frac{L_q}{L_d} \\ -p\omega_r \frac{L_d}{L_q} & -\frac{R_S}{L_q} \end{bmatrix} \cdot \begin{bmatrix} i_d \\ i_q \end{bmatrix} - \frac{p\omega_r}{L_q}\begin{bmatrix} 0 \\ \Phi_{PM} \end{bmatrix} + \begin{bmatrix} \frac{1}{L_d} & 0 \\ 0 & \frac{1}{L_q} \end{bmatrix} \cdot \begin{bmatrix} u_d \\ u_q \end{bmatrix} \quad (2.1), (2.2)$$

$$\frac{d\omega_r}{dt} = \frac{1}{J}\left\{ c_5\left[ \Phi_{PM} i_q + \left(L_d - L_q\right) i_d\, i_q \right] - \Gamma_L \right\} = \frac{1}{J}\left\{ \Gamma_{el} - \Gamma_L \right\} \quad (2.3)$$

where $i_d$, $i_q$ and $u_d$, $u_q$ are, respectively, the stator current and voltage components, p is number of polpairs, $\omega_r$ is the rotor angular velocity, $\Phi_{PM}$ is magnetic flux of permanent magnets, $\Gamma_L$ is the external load torque and $c_5$=1.5*p.

**Master control law** is based on *linearising function* [9], which forces a non-linear system to obey specified linear closed-loop differential equations:-

$$\frac{d\omega_r}{dt} = \frac{1}{T_1}\left(\omega_d - \omega_r\right) \quad (2.4)$$

Equation (2.3) for the rotor velocity is made to follow equation (2.4) by equating their right hand sides:-

$$\frac{1}{J}\left\{ c_5\left[ \psi_d i_q - \psi_q i_d \right] - \Gamma_L \right\} = \frac{1}{T_1}\left(\omega_d - \omega_r\right) \quad (2.5)$$

The rotor magnetic flux calculator estimates the individual rotor flux components, $\Psi_d$ and $\Psi_q$ :-

$$\begin{cases}\psi_d^* = \tilde{L}_d\, i_d + \tilde{\Psi}_{PM} \\ \psi_q^* = \tilde{L}_q\, i_q\end{cases} \qquad (2.6)$$

The second part of the control law is formulated as vector control on the basis of PMSM construction which has the magnets mounted on the rotor surface. Maximum torque sensitivity [1] is achieved with:-

$$i_d = 0 \qquad (2.7)$$

Taking into account equations (2.6), (2.7) and (2.5) corresponding $i_q$ can be found. Computed two current components are then used to generate the *demanded* values of $i_d$ and $i_q$ which are denoted as $i_{d\_dem}$ and $i_{q\_dem}$ In real control law the state variables and motor parameters are replaced by their estimates as will be the case in practise:-

$$\begin{cases} i_{d\_dem} = 0 \\ i_{q\_dem} = \dfrac{1}{c_5 \Phi_{PM}}\left[\hat{\Gamma}_L + \dfrac{\tilde{J}}{T_1}\left(\omega_d - \omega_r^*\right)\right] \end{cases} \qquad (2.8)$$

**State Estimation and Filtering**

**The pseudo sliding mode observer and angular velocity extractor** Pseudo sliding-mode observer used here is based on stator current equations (2.1) and (2.2). The real time model of this system fed by actual stator voltages and real stator currents is developed but *purposely using only the terms without rotor speed, $\omega_r$*. Thus:-

$$\frac{d}{dt}\begin{bmatrix} i_d^* \\ i_q^* \end{bmatrix} = \begin{bmatrix} \dfrac{1}{\tilde{L}_d} & 0 \\ 0 & \dfrac{1}{\tilde{L}_q} \end{bmatrix} \cdot \begin{bmatrix} u_d \\ u_q \end{bmatrix} + \begin{bmatrix} v_{eq\ d} \\ v_{eq\ q} \end{bmatrix} \qquad (2.9)$$

where $v_{eq\ d}$ and $v_{eq\ q}$ are the model corrections and $i^*_d$ and $i^*_q$ are estimates of $i_d$ and $i_q$ as in a conventional observer. The useful observer outputs here are the continuous *equivalent values* of the rapidly switching variables:-

$$\begin{bmatrix} v_{eq\ d} \\ v_{eq\ q} \end{bmatrix} = V_{max}\, \mathrm{sgn}\begin{bmatrix} i_d - i_d^* \\ i_q - i_q^* \end{bmatrix} \qquad (2.10)$$

Equation (2.10) cannot directly generate $v_{eq\ d}$ and $v_{eq\ q}$. Instead, a *pseudo-sliding-mode* observer [11] may be formed by replacing equation (2.10) with (2.11):-

$$\begin{bmatrix} v_{eq\ d} \\ v_{eq\ q} \end{bmatrix} = K_{sm}\begin{bmatrix} i_d - i_d^* \\ i_q - i_q^* \end{bmatrix} \qquad (2.11)$$

where the gain, $K_{sm}$, is made as high as possible within the stability limit. For large $K_{sm}$, the errors between real motor currents and fictitious observer currents are driven almost to zero with the result yielding (2.12):-

$$\begin{bmatrix} v_{eq\ d} \\ v_{eq\ q} \end{bmatrix} = \begin{bmatrix} \dfrac{-\tilde{R}_s}{\tilde{L}_d} & p\omega^*_r \dfrac{\tilde{L}_q}{\tilde{L}_d} \\ -p\omega^*_r \dfrac{\tilde{L}_d}{\tilde{L}_q} & \dfrac{-\tilde{R}_s}{\tilde{L}_q} \end{bmatrix} \cdot \begin{bmatrix} i_d \\ i_q \end{bmatrix} - \frac{p\omega^*_r}{\tilde{L}_q}\begin{bmatrix} 0 \\ \tilde{\Phi}_{PM} \end{bmatrix} \qquad (2.12)$$

Based on equation (2.12) an unfiltered angular rotor velocity estimate, $\omega_r^*$, can be extracted. The component which has minimal noise distortion (2.13), including special numerical algorithm described in [10] is used for additional filtering.

$$\omega_r^* = \frac{-\tilde{L}_q v_{eq\ q} - R_s\, i_q}{p \cdot \left(\tilde{L}_d\, i_d + \tilde{\Phi}_{PM}\right)} \qquad (2.13)$$

**Observer for Load Torque Estimation and Rotor Speed Estimate Filtering:** The load torque estimate required by the master control law is provided here by a standard observer having a similar structure to a Kalman filter, a direct measurement of this variable being assumed to be unavailable. The real time model of this observer is based on torque equations (2.3). The observer correction loop is actuated by the error between the rotor speed estimate, $\omega^*_r$, from the angular velocity extractor of previous section and the estimate, $\hat{\omega}_r$, from the real time model.

$$\begin{cases} e_\omega = \omega_r^* - \hat{\omega}_r \\ \dot{\hat{\omega}}_r = \frac{1}{\tilde{J}}\left(\tilde{c}_5\left[\tilde{\Phi}_{PM}\, i_q + \left(\tilde{L}_d - \tilde{L}_q\right) i_d\, i_q\right] - \hat{\Gamma}_L\right) + k_\omega e_\omega \\ \dot{\hat{\Gamma}}_L = k_\Gamma\, e_\omega \end{cases} \qquad (2.14)$$

Since $\hat{\omega}_r$ is a filtered version of $\omega^*_r$ it is used directly in the master control law. This is a conventional second order linear observer with a correction loop characteristic polynomial, which may be chosen via the gains, $k_\omega$ and $k_\Gamma$, to yield the desired balance of filtering between the noise from the measurements of currents $i_d$ and $i_q$ and the noise from the velocity measurement, $\omega^*_r$.

### 2.2. The inner control loop

Bang-bang control based inner control loop forces the real stator currents, $i_a$, $i_b$ and $i_c$, to follow corresponding master control law current demands, $i_{a\_dem}$, $i_{b\_dem}$,and $i_{c\_dem}$, as closely as possible. This is done by switching the power electronic switching state to an appropriate value upon every iteration

interval of the digital processor. The *bang-bang* type slave control law is then:-

$$u_j = U_s \operatorname{sgn}\left(i_{j\,dem} - i_j\right), \quad j=1, 2, 3 \qquad (2.15)$$

The effect of this is similar to the standard hysteresis controller, but the hysteresis element is unnecessary because the maximum power electronic switching frequency is automatically limited to 1/h, where h is the iteration interval of the control algorithm. Thus, the motor is current fed. This is important as it eliminates the stator time constant from the problem of designing the outer loop controllers.

### 2.3. Sliding Mode Outer Loop Controller

Sliding mode control is a type of bang-bang control in which the plant state is forced towards and maintained within a close vicinity of a boundary determined by the control system designer. If for a single input, single output plant the state variables are chosen as the controlled output and its derivative up to n-1 (*n is rank of plant*), then if the state is maintained precisely on the boundary, the closed loop dynamics is determined by the boundary and is independent of the plant parameters and external disturbances [11].

Since the proposed middle loop controller is model based (*it contains algorithms depending on estimates of the rotor angular speed and load parameters*) the closed-loop performance will be affected by errors in these estimates. The purpose of the outer loop controller is to improve robustness of the overall control system against uncertain parameters and external load torque, $\Gamma_L$. The closed-loop system created by the inner and middle control loops has the ideal nominal transfer function (2.16):-

$$\frac{\hat{\omega}_r(s)}{\omega_d(s)} = \frac{1}{1+sT_\omega} \qquad (2.16)$$

Let the errors introduced by the motor parameter uncertainties, external load torque and imperfect operation of the middle control loop due to the non-zero iteration interval are approximately represented by a change of DC gain, $K_d$ and time constant, $T'_\omega$. Then the combined inner and middle loop dynamics may be again represented by the new transfer function (2.17), where $K_d > 0 \,\&\, \neq 1$ and $T'_\omega > 0 \,\&\, \neq T_\omega$:-

$$\frac{\hat{\omega}_r(s)}{\omega'_d(s)} = \frac{K_d}{1+sT'_\omega} \qquad (2.17)$$

Consider now the introduction of a pure integrator and a high gain element with saturation at the speed reference input of the middle loop as it is shown in Fig.3. New control variable of the real system now is $\omega'_d$ as the outer loop output. The input of inserted integrator is also treated as a new control variable, $u'$.

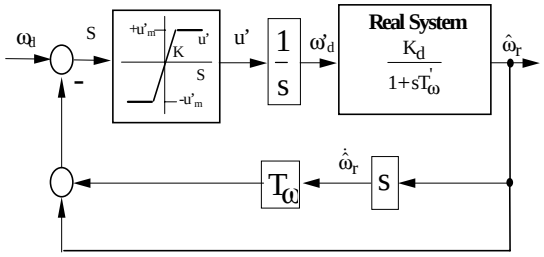


Fig. 3: Sliding mode based outer control loop.

If the gain, K, is infinite, then the transfer characteristic between S and $u'$ yields the bang-bang control:-

$$u' = u'_m \operatorname{sign}(S) \qquad (2.18)$$

where

$$S = \omega_d - \hat{\omega}_r - T_\omega \dot{\hat{\omega}}_r \qquad (2.19)$$

The output derivative, $\dot{\hat{\omega}}_r$, may be obtained without differentiation by using the second of equations of filtering observer (2.14). If conditions for sliding mode are fulfilled and ones the switching boundary is reached, the state trajectory is maintained close to it, while the control variable $u'$, rapidly switches between values of $+u'_m$ and $-u'_m$ for S=0. Setting this condition in equation (2.19) then yields the switching boundary. Under these circumstances, the closed-loop system obeys the switching boundary equation done by (2.20) and this corresponds to transfer function (2.17) with $K_d$=1 and $T'_\omega$=$T_\omega$.

$$\dot{\hat{\omega}}_r = \frac{1}{T_\omega}\left(\hat{\omega}_r - \omega_d\right) \qquad (2.20)$$

This means that without parameter uncertainties or external load torque, the outer loop controller makes no difference to the closed-loop dynamics. It merely compensates for the effects of the parameter mismatches and load torque, thereby yielding the required robustness.

The control chatter of the design system would interact in an undesirable way with the switching of the power electronics elements. This can be eliminated by the reducing slope of the high gain element, K, to a finite but still relatively large value and removing saturation limits. Then it may be shown that for $K \to \infty$ also $S \to 0$ and therefore the resulting performance is similar to the described classical sliding mode controller and this also yields similar robustness.

## 3. SIMULATIONS AND EXPERIMENTAL RESULTS

The theory presented was verified by simulation with intention to investigate robustness of the design control system with respect to the load torque. For comparison the simulations were carried out without and then with outer control loop for prescribed time constant $T_\omega$=0.1 s. All simulations started with zero initial states and a step rotor speed demand $\omega_d$=70 rad/s. A step disturbance nominal torque of $\Gamma_L$=3 Nm was applied for t=0.4 s, when steady state of idle running motor was already achieved.

In all the simulations presented, the stator current $i_\alpha$ and $i_\beta$ components during the starting interval $t \in$ (0-0.2) s as functions of time are shown in subplots (a). The magnetic flux components $\Psi_\alpha$ and $\Psi_\beta$ as functions of time for the same interval, $t \in$ (0-0.2) s are shown as subplot (b). Subplot (c) shows the speed estimate, $\hat{\omega}_r$, and load torque estimate, $\hat{\Gamma}_L$, from the filtering observer together with ideal speed response $\omega_{id}$ (*dashed line)* computed from transfer function. Finally, subplot (d) shows the angular rotor speed, $\omega_r$, together with ideal speed response $\omega_{id}$ (*dashed line*). These two angular speeds are also presented for experiments.

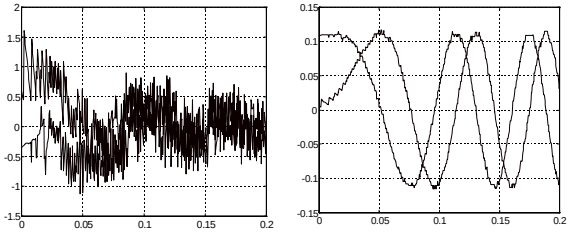

a) $i_\alpha$, $i_\beta$=f(t) b) $\Psi_\alpha$, $\Psi_\beta$=f(t)

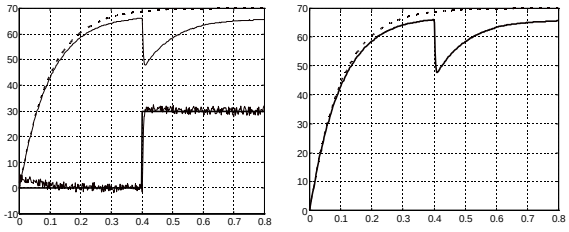

e) $\omega_{id}$, $\hat{\omega}_r$, $\Gamma_L$, $\hat{\Gamma}_L$=f(t) f) $\omega_{id}$, $\omega_r$= f(t)

Fig.4. Simulated speed response and corresponding variables without SMC outer loop.

The basic effect of the sliding mode based outer loop may be observed from simulation presented as Fig. 5. The improvement brought about when SMC outer loop is applied is clearly evident. Previous approximately 7% error of angular speed in steady state visible from Fig. 4 was completely eliminated and speed reduction due to applied nominal load torque at t=0.4 s is also less significant.

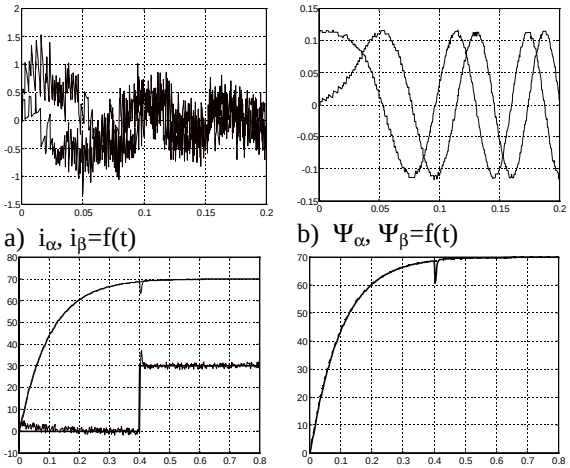

a) $i_\alpha$, $i_\beta$=f(t) b) $\Psi_\alpha$, $\Psi_\beta$=f(t)



c) $\omega_{id}$, $\hat{\omega}_r$, $\hat{\Gamma}_L$=f(t) d) $\omega_{id}$, $\omega_r$= f(t)

Fig.5. Simulated speed response and corresponding variables together with SMC outer loop.

For experiments the control algorithms were also implemented on a Pentium PC equipped with PC Lab card. The stator currents are measured through LEM transformers and evaluated using a PC Lab Card PL818. A six-transistor Semikron IGBT module was used as the three-phase inverter controlled via PC. All the experiments presented were carried out with a DC supply voltage of $U_{DC}$=90 V and step rotor speed demands of $\omega_{dem}$=200 rad/s and a time constant of $T_\omega$=0.15 s. Data logging of the experimental variables was carried out for a 1.8 s time interval. The PMSM was idle running during all the experiments.

The experimental results obtained with the middle and inner control loops, excluding the SMC loop, are shown in Fig. 6. The errors between the ideal angular speed and the estimated and real angular speeds due to imperfections in estimations and non-zero iteration interval even in the steady-state are clearly visible. It was also reason that the drive without outer control loop was originally design for moderate accuracy.

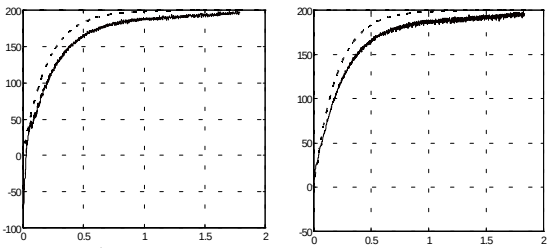

a) $\omega_{id}$, $\hat{\omega}_r$, = f(t) b) $\omega_{id}$ , $\omega_r$=f(t)

Fig. 6. Experimental results - ideal speed response compared with observed and real speed without SMC outer loop.

Experimental results corresponding to those of Fig.6, but including the SMC based outer loop, are shown in Fig.7. The significant reduction of the aforementioned errors brought about by the SMC based outer loop, both during the acceleration of the drive and in the steady state, is evident by comparison of these two figures. Finally, the

experimental results presented show good correspondence with theoretical predictions and here presented simulations.

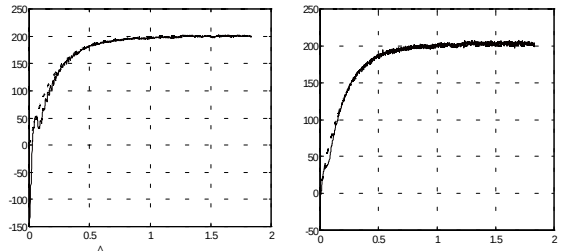

a) $\omega_{id}$, $\hat{\omega}_r$, = f(t) b) $\omega_{id}$ , $\omega_r$=f(t)

Fig. 7. Experimental results - ideal speed response compared with observed and real speed with SMC outer loop.

## 4. CONCLUSIONS AND RECOMMENDATIONS

The presented simulation and also experimental results (for an unloaded PMSM) confirm that the addition of a SMC based outer control loop to the forced dynamics shaft sensorless speed control system considerably improves its performance. The SMC loop also rendered the starting position of PMSM less critical.

Suggestions for future research work are:

- an investigation of robustness and effectiveness of SMC outer control loop with respect to motor and load parameter uncertainties,
- application of more sophisticated inverter control strategy such as '*Space Vector Modulation*', which can improve shape of current components and secondary will affect also activity of observers too.
- a further set of experimental trials, including application of step load torque, together with an extensive investigation of the variation of the filtering observer performance with the pole locations.

## 5. REFERENCES


[1] Boldea, I., Nassar, A.S.: 'Vector Control of AC Drives', ***CRC Press*** London 1992.

[2] Bose B.: Power Electronics and AC Drives. ***Ed. Prentice Hall,*** Englewood Cliffs, 1986.

[3] Dodds, S.J. Utkin, V.A., Vittek, J.: 'A Motion Separation Method for the Control of Induction Motors with Prescribed Closed-Loop Dynamics', ***NOLCOS'95****:* IFAC Conference, Tahoe City, California, Vol.2, pp.816-821.

[4] Dodds, S.J, Utkin, V.A., Vittek, J.: 'Self Oscillating, Synchronous Motor Drive Control System with Prescribed Closed-Loop Speed Dynamics'. Proceedings of ***2nd EPE Chapter Symposium***, Nancy, France, June 1996, pp.23-28.

[5] Dodds, S.J., Vittek, J.: 'Synchronous Motor Drive with Prescribed Closed-loop Speed Dynamics Employing a Two-phase Oscillator'. Proceedings of ***EDPE'96*** Conference, High Tatras, Sept. 1996, pp.209-216.

[6] Dodds, S.J., Vittek, J., Seman, S.: 'Implementation of a Sensorless Synchronous Motor Drive Control System with Prescribed Closed-Loop Speed Dynamics'. Proceedings of ***SPEEDAM'98***, Sorrento, Italy, June 1998, pp. P4-5 - P4-10.

[7] Dodds, S.J., Vittek, J.: Robust Cascade Forced Dynamics Control of Shaft Sensorless Synchronous Motor Drive'. Proceedings of ***ELECTROMOTION'99*** Conference, Patras, Greece, June 1999, pp.447-452.

[8] Dodds, S.J., Vittek, J.: 'Near-Time-Optimal Position Control Of Electrical Drives Based On Forced Dynamics Control'. Proceedings of ***ELECTRO'99*** Faculty of Electrical Engineering Conference, University of Zilina, Slovakia, May 1999, pp.108-116.

[9] Isidori, A.: 'Nonlinear Control Systems'. 2nd edition, ***Springer-Verlag*** Berlin, 1990.

[10] Korondi, P., Young, D.K., Hashimoto, H.: Sliding Mode Based Disturbance Compensation for Motion Control. Proceedings of ***IEEE-IECON'97*** Conference, New Orleans, Louisiana, Nov. 1997, pp.73-78.

[11] Utkin, V.I.: 'Sliding Modes in Control and Optimisation'. ***Springer Verlag*** Berlin, 1992.


## Appendix

The PMSM parameters are as follows:- $P_n$=475 W; at $\omega_n$=157 rad/s, p=2; $R_S$=1.26 Ω, $L_d$=9.34 mH; $L_q$=9.2 mH; $\Phi_{PM}$ =0.112 Vs and the lumped moment of inertia is J=0.0005 kgm$^2$.


**Acknowledgements**

The authors wish to thank the **European Commission, Brussels**, for funding the **INCO COPERNICUS** programme **No.960169** '**Ucodrive'** and **Slovak Grant Agency VEGA** for funding research programme **No. 1/6111/99**. We would like also to thank our colleagues Seman, S., Vanko, D. and Rosko, P. of Zilina University, for producing the experimental results for PMSM drive with forced dynamics and sliding mode based outer control loop.